JOURNAL OF Materials CHEMISTRY

Structural characterization and physical properties of $LaNi_{1-x}Mo_xO_3$ ($0.05 \leqslant x \leqslant 0.20$) perovskites

Elizabeth Rodríguez,[a] Inmaculada Álvarez,[a] María Luisa López,*[a] María Luisa Veiga,[a] Carlos Pico[a] and José Luis Martínez[b]

[a]*Departamento de Química Inorgánica I, Facultad de Ciencias Químicas, Universidad Complutense, 28040 Madrid, Spain. E-mail: marisal@eucmax.sim.ucm.es*
[b]*Instituto Ciencia de Materiales de Madrid, CSIC, Cantoblanco, 28049 Madrid, Spain*

Received 4th July 2000, Accepted 22nd September 2000
First published as an Advance Article on the web 1st December 2000

The structural characterization and physical properties of the $LaNi_{1-x}Mo_xO_3$ ($0.05 \leqslant x \leqslant 0.20$) perovskite-like system are reported. These compounds can be regarded as being derived from $LaNiO_3$ by partial substitution in the B sublattice of the perovskite structure: Ni^{3+} by Mo^{6+} with the consequent reduction of some Ni^{3+} to Ni^{2+}. Rhombohedral (S.G. $R\bar{3}c$) or orthorhombic (S.G. *Pbnm*) symmetry was found depending on the degree of substitution, x.

Conductivity measurements show the presence of metal-to-insulator (M–I) transitions in these oxides. Magnetic properties show weakly ferromagnetic ($x = 0.05$) to antiferromagnetic with very weak ferromagnetic canting ($x = 0.20$), respectively.

Introduction

The $RNiO_3$ perovskites (R = rare-earth) have been extensively studied in the last few years[1–4] because they show metal-to-insulator (M–I) transitions as a function of temperature, that systematically vary with the rare-earth size. The occurrence of these thermally driven M–I transitions has been related to the closing of the charge-transfer gap, induced by the narrowing of the electronic bandwidth when temperature decreases.[5,6]

The degree of distortion of the structure determines the onset of electronic localization: for a given R^{3+} size the NiO_6 octahedra are tilted in order to optimize R–O bond distances, giving rise to bent Ni–O–Ni angles determining the degree of overlapping of Ni 3d and O 2p orbitals and, therefore, the electronic bandwidth.

In this context, some systems such as $LaNi_{1-x}M_xO_3$ (M = Cr, Mn, Fe, Co, Cu, Sb)[7–9] and $La_{n+1}Ni_nO_{3n+1}$,[10] in which Ni cations are present in mixed-valent states, show interesting electrical and magnetic properties that could be qualitatively related to the relative amounts of Ni^{2+} and Ni^{3+}. In order to interpret the magnetic behaviour, the probability of antiferro- or ferro-magnetic interactions and the evolution of electronic localization in the systems have been taken into account.

The attractive electronic and magnetic properties displayed by this kind of material have prompted us to prepare and study some perovskite-type oxides in which nickel cations are present in mixed-valent states to evaluate the main features involved in their physical properties. In this respect, we have previously reported structural, magnetic and electronic results for the $LaNi_{1-x}W_xO_3$ system[11–13] and $LaNi_{1-x}Ti_xO_3$[14] in which an M–I transition has also been observed and we have analysed the influence of the nature of cations located on the B sites of perovskite on both kinds of properties. In this paper, we complete this study and report the structural characterization and electrical and magnetic behaviour of the series $LaNi_{1-x}Mo_xO_3$ between the compositional limits of $x = 0.05$ and 0.20. The upper limit of this series, $x = 0.25$, for which the nickel content should be present as Ni^{2+}, could not be isolated as a pure phase.

Experimental

The title oxides were prepared by the "liquid mix" technique.[15] The synthesis was carried out in air, starting from $La(NO_3)_3{\cdot}6H_2O$, $Ni(NO_3)_2{\cdot}6H_2O$ and MoO_3 (supplied by Fluka, Panreac and Merck, respectively). The temperature employed in the synthesis ranged between 723 and 1073 K for several days, as described elsewhere.[11] During the thermal treatment, the samples were reground in each step and the process was monitored by X-ray diffraction until single and pure phases were obtained. The X-ray diffraction patterns were recorded with a Philips X'Pert-MPD diffractometer with a PW 3050/00 goniometer, using Ni-filtered Cu-Kα and a 2θ step size of 0.05° with a counting time of 12.5 s for each step. The goniometer was connected to a PC controlled by the commercial program PC-APD (Analytical Powder Diffraction Software, 4.0 e).

Neutron powder diffraction data were recorded at room temperature on the D1A high-resolution powder diffractometer ($\lambda = 1.9110$ Å) at the Institut Laue-Langevin (Grenoble, France). The neutron and X-ray diffraction patterns were analyzed through the Rietveld method by the Fullprof program.[16] A pseudo-Voigt function was chosen to generate the lineshape of the diffraction peaks.

Electrical conductivity measurements were registered on pelletized samples sintered at 1073 K for 48 h in air, using a d.c. four probe apparatus according to the Van der Pauw method.[17] Colloidal platinum paint was used to make contacts. Magnetic susceptibility data were obtained with a SQUID (Quantum Design, MPMS-XL model) in the temperature range 2–300 K in an applied magnetic field of 1000 Oe in all ZFC measurements.

Results and discussion

Structural characterization

X-Ray diffraction (XRD) data for all the title compounds were analyzed by means of the Rietveld method. The parent phase $LaNiO_3$, *i.e.* $x = 0$, was found to have a rhombohedrically distorted perovskite structure, S.G. $R\bar{3}c$ (no. 167), whose

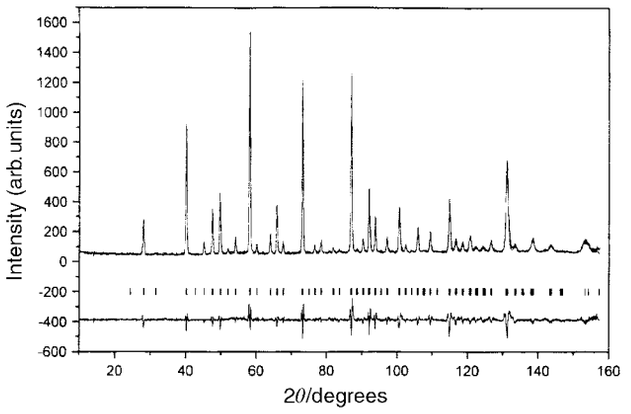

Fig. 1 Observed (dots) and calculated (solid line) neutron diffraction profiles for the orthorhombic $LaNi_{0.80}Mo_{0.20}O_3$ at room temperature.

hexagonal parameters were $a=5.446(1)$ Å and $c=13.154(2)$ Å, as was previously reported.[11]

The diffraction data for the less substituted sample, $x=0.05$, were refined considering a rhombohedral symmetry and the same space group $R\bar{3}c$. On the other hand, XRD patterns for the rest of the series, $LaNi_{1-x}Mo_xO_3$ ($0.10 \leqslant x \leqslant 0.20$), showed that a structural transition took place and they could be indexed and refined considering an orthorhombic symmetry (unit cell of size $\sqrt{2}a_0 \times \sqrt{2}a_0 \times 2a_0$ and space group *Pbnm*, no. 62). The structure refinements for the $LaNi_{0.8}Mo_{0.2}O_3$ compound were made separately from X-ray diffraction and neutron diffraction (ND). On the basis of the good agreement between both sets of results, this structural model was chosen for the remaining compositions whose XRD results will be discussed.

Fig. 1 shows the observed and calculated neutron diffraction profiles for $LaNi_{0.8}Mo_{0.2}O_3$, at room temperature, and in Table 1 the crystal data and agreement factors are gathered (last column, $x=0.20$, ND). The refinement of the O1 and O2 occupancy factors shows that the oxygen positions are fully occupied and, therefore, the stoichiometry of this compound could be effectively assumed. From the agreement between the observed and calculated profiles as well as the *R*-factors obtained one can accept as valid the proposed model. In order to evaluate the distortion within a $(Ni/Mo)O_6$ octahedron, interatomic distances were calculated and are listed in Table 2. There are three different (Ni/Mo)–O pairs of distances in the octahedron and, as can be seen, the distortion within an $(Ni/Mo)O_6$ octahedron is rather considerable. The average of the three distances agrees well with the Shannon ionic radii sums, that varies between 1.98 and 2.04 Å for both compositional limits, $x=0.05$ and $x=0.20$, respectively (calculated on the assumption that the Ni^{3+} cations in octahedral coordination maintain the low-spin electronic configuration, $t_{2g}^6 e_g^1$). The values of the La–O bond distances vary over a wide range, indicating that the La–O polyhedron is quite distorted, and can be described as a bicapped trigonal prism. Therefore, the coordination number of La decreases from 12 in the aristotype to 8 in this phase. The void is reduced in size by tilting of the octahedra and the actual values of the (Ni/Mo)–O–(Ni/Mo) angles can be used to evaluate such a tilting. These values are included in Table 2 and are significantly lower than the ideal angle of 180°, showing that the octahedral tilt is relatively large. This fact will be decisive in the physical properties of the title materials, as discussed below.

Table 1 also shows crystallographic data for the remaining compositions ($x=0.05$–0.15). An examination of refined atomic coordinates indicates that Ni and Mo are placed on the ideal perovskite B sites and the other atoms (La, O1 and

Table 1 Refined crystal data and *R*-factors for $LaNi_{1-x}Mo_xO_3$

$LaNi_{1-x}Mo_xO_3$	$x=0.05$ (XRD)	$x=0.10$ (XRD)	$x=0.15$ (XRD)	$x=0.20$ (XRD)	$x=0.20$ (ND)
a/Å	5.472(1)	5.443(1)	5.519(1)	5.5534(6)	5.5512(3)
b/Å	5.472(1)	5.496(1)	5.528(1)	5.5645(6)	5.5614(3)
c/Å	13.204(1)	7.769(1)	7.807(2)	7.8482(9)	7.8430(4)
V/Å^3	342.51(1)	232.45(1)	238.11(1)	242.52(1)	242.13(2)
La					
x	0	−0.004(1)	0.0058(4)	−0.0101(4)	0.010(2)
y	0	−0.0138(6)	−0.0263(7)	−0.0321(2)	−0.0305(9)
z	0.25	0.25	0.25	0.25	0.25
B/Å^2					1.68(5)
Ni					
x	0	0.5	0.5	0.5	0.5
y	0	0	0	0	0
z	0	0	0	0	0
B/Å^2					0.25(5)
Mo					
x	0	0.5	0.5	0.5	0.5
y	0	0	0	0	0
z	0	0	0	0	0
B/Å^2					0.25(5)
O1					
x	0.539(2)	0.23(1)	0.213(0)	0.218(5)	0.216(1)
y	0	0.25(1)	0.225(4)	0.214(4)	0.211(1)
z	0.25	0.031(3)	0.025(1)	0.028(2)	0.0395(8)
B/Å^2					0.8(1)
Occupation					8.2(2)
O2					
x		0.00(1)	−0.065(8)	−0.061(7)	−0.067(2)
y		−0.485(6)	−0.495(1)	−0.493(2)	−0.487(1)
z		0.25	0.25	0.25	0.25
B/Å^2					0.7(3)
Occupation					3.8(2)
R_F	6.29	8.53	8.34	10.4	3.79
R_B	8.71	9.29	7.27	8.20	5.18
R_P	10.9	10.5	9.32	10.1	10.8
R_{WP}	14.0	14.2	12.8	13.4	13.5
χ^2	9.32	7.85	2.69	3.93	3.63

Table 2 Interatomic distances (Å) and angles (°) for $LaNi_{1-x}Mo_xO_3$

$LaNi_{1-x}Mo_xO_3$	$x=0.05$ (XRD)	$x=0.10$ (XRD)	$x=0.15$ (XRD)	$x=0.20$ (XRD)	$x=0.20$ (ND)
La–O1	2.519(0)	2.598(7) ×2	2.515(4) ×2	2.552(4) ×2	2.414(6) ×2
	2.953(5)	2.584(7) ×2	2.714(8) ×2	2.758(5) ×2	2.659(2) ×2
	2.519(2) ×2	2.842(3) ×2	2.699(2) ×2	2.677(5) ×2	2.787(2) ×2
	2.953(8) ×2				
	2.717(8) ×2				
	2.717(8) ×2				
	2.717(9) ×2				
La–O2		2.596(2)	2.621(0)	2.584(4)	2.578(2)
		2.715(5)	2.434(6)	2.387(6)	2.474(1)
Mean	*2.73*	*2.66*	*2.61*	*2.62*	*2.60*
Ni/Mo–O1	1.937(5) ×3	2.012(8) ×2	2.025(3) ×2	1.981(2) ×2	1.990(3) ×2
	1.937(6) ×3	1.886(3) ×2	1.929(6) ×2	2.010(1) ×2	2.028(2) ×2
Ni/Mo–O2		1.944(3) ×2	1.985(5) ×2	1.992(0) ×2	1.997(1) ×2
Mean	*1.94*	*1.95*	*1.98*	*1.99*	*2.005*
Ni/Mo–O1–Ni/Mo	167.1	165.4	161.9	160.0	155.7
Ni/Mo–O2–Ni/Mo		174.9	158.8	160.1	158.0

O2) are slightly displaced from their respective ideal positions. A comparison of the atomic coordinates obtained for all compositions show that La, O1 and O2 atoms are more displaced from their ideal sites when x increases. As a consequence of this fact, the $(Ni/Mo)O_6$ octahedra are quite distorted as can be seen in Table 2. The orthorhombic samples show three different $(Ni/Mo)O_6$ sets of bond distances, whereas in the rhombohedral one ($x=0.05$) the corresponding six bond lengths are close to 1.93 Å, a value that is very similar to those in the parent phase, $LaNiO_3$.[11] Moreover, it is interesting to note that the interatomic distances between the Ni/Mo and the apical oxygen O2 atoms decrease for lower x values.

On the other hand, the octahedral tilt is smaller when x decreases, being higher than the Ni/Mo–O–Ni/Mo angles in this sense, although this effect is less marked in the Ni/Mo–O1–Ni/Mo angles variation. The rhombohedral phase ($x=0.05$) shows a unique M–O–M angle that is significantly different from the ideal value of 180° by *ca.* 13°, showing that the octahedral tilt remains relatively large in this structure.

In the orthorhombic samples, the La coordination number is 8 whereas for the rhombohedral one the La–O distances suggest a coordination number 12 for La ion, as occurs in the parent compound, $LaNiO_3$.[11]

Conductivity measurements

The electronic conductivity variation with temperature for the $LaNi_{1-x}Mo_xO_3$ perovskites has been measured in the temperature range 5–400 K and up to 1123 K for $x=0.10$ by the four probe method.[17]

Fig. 2 shows the variation of ln σ *vs.* T^{-1} and these results suggest that the conductivity is dependent on the composition. As a general trend for all phases, the conductivity values are lower as x increases and this fact seems to be a consequence of the progressive localization of the atomic levels or, alternatively, the progressive decreasing of the bandwidth. The materials with $x \leqslant 0.10$ show a metal-to-insulator (M–I) transition at low temperatures (40 K for $x=0.05$ and 160 K for $x=0.10$) as can be seen in Fig. 3, which can be related to the increase in electronic correlations as a consequence of doping.[8] The behaviour of samples $x=0.05$ and $x=0.10$ can be interpreted as in $LaNiO_3$[10,18] where a conduction band is built from the hybridization of the e_g nickel semioccupied orbitals (in low spin configuration) and oxygen orbitals. In this sense, such a material can be classified as a low "w" semimetal (where "w" is the bandwidth), *i.e.* a highly correlated metal.

The conductivity value obtained for $x=0.15$ at room temperature is 61.58 S cm^{-1}. This is a low value for conductivity of a metal and this fact, together with the enhancement of conductivity above 100 K, can been interpreted in terms of an important electronic localization. At high temperatures (100–400 K) the activation energy was 0.05 eV which is characteristic of semimetallic behaviour.

The compound of composition $LaNi_{0.80}Mo_{0.20}O_3$ behaves as a semiconductor in whole temperature range studied. The conductivity data for this material were fitted to an exponential law as:

$$\sigma = \left(\frac{A}{T}\right) \exp\left(\frac{E}{KT}\right) \quad (1)$$

which is usually applied to a small polaron hopping mechanism. In eqn. (1), E is the activation energy related to the hopping process, A is the pre-exponential factor and K is the Boltzmann constant. The activation energy obtained for this

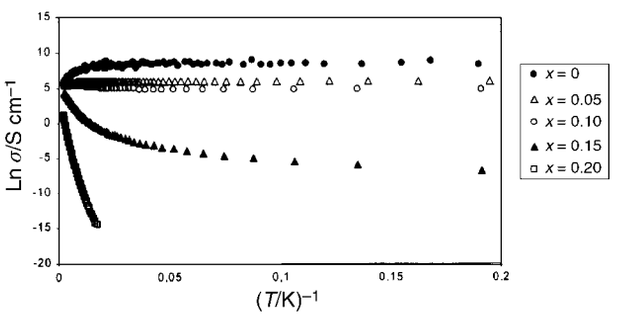

Fig. 2 Variation of ln σ *vs.* T^{-1} for $LaNi_{1-x}Mo_xO_3$ in the 5–400 K temperature range.

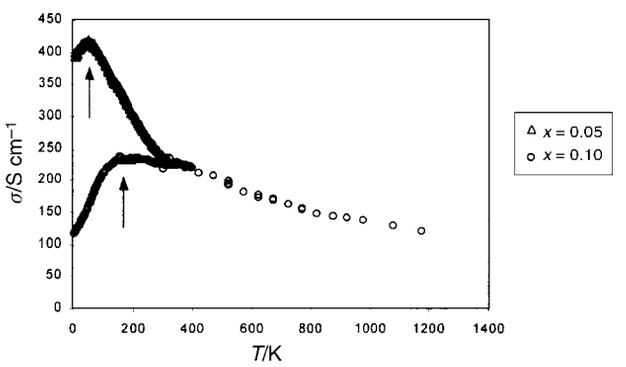

Fig. 3 Variation of conductivity *vs.* temperature for $LaNi_{1-x}Mo_xO_3$ for the $x=0.05$ and $x=0.10$ compounds.

material was $E_a = 0.11$ eV, which agrees well with the above assumption.

The observed electronic behaviour can be qualitatively explained bearing in mind the dependence of B–O1–B and B–O2–B values on composition for these mixed oxides. As was discussed above, when x decreased these angles increased and, in this sense, the overlapping between Ni/Mo d orbitals with the oxygen p orbitals is more effective, giving rise to wider bands which are responsible for the progressive tendency towards metallic behaviour. Similar results have been previously reported for other systems derived from $RNiO_3$ (R = rare-earth) perovskites.[19]

When $x = 0.20$ the system rises to the limit of the insulating side of this transition, and the conduction process could occur *via* a hopping mechanism for which the activation energy is close to 0.11 eV. This mechanism would suggest the presence of an important electronic localization as a consequence of the lattice polarization.

Magnetic measurements

Fig. 4(a) shows the variation of magnetic susceptibility for the temperature range 1.9–300 K in a magnetic field of 1000 Oe, for $x = 0.05$. An almost temperature-independent behaviour is observed above ~35 K, consistent with Pauli paramagnetism with $\chi_{RT} \sim 10^{-3}$ emu mol^{-1} (where RT designates room temperature), and this can be related to the existence of an important electronic delocalization above this temperature. This enhanced χ value indicates a relatively strong correlation among the 3d electrons in a narrow band as was reported earlier for the $x = 0$ phase[20] as well as for a similar compound such as $LaNi_{1-x}W_xO_3$.[12] Below ~35 K, a marked enhancement of magnetization values with decreasing temperature is observed, which, in principle, can be associated with ferromagnetic interactions, as in $LaNiO_3$.[20]

Fig. 4(a) also shows the variation of magnetic susceptibility for the same magnetic field of 1000 Oe for compositions $x = 0.10$ and 0.15. In both cases different behaviour is evidenced and a paramagnetic region appears above

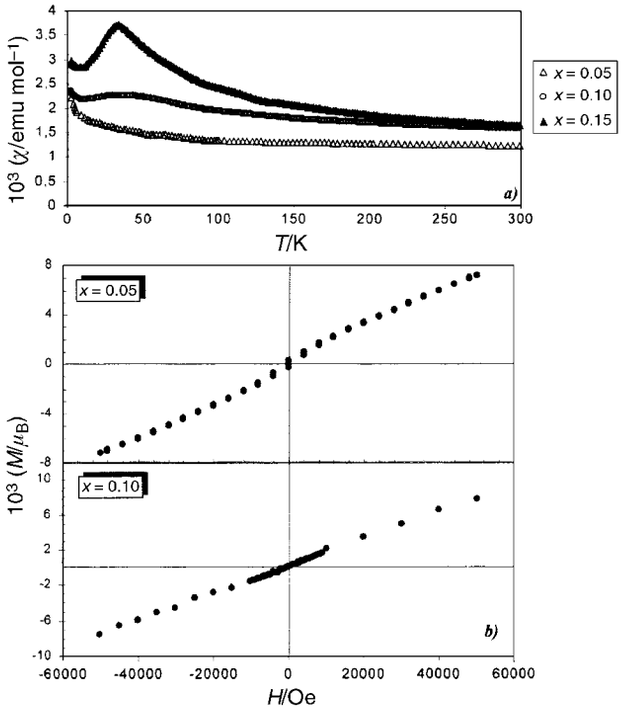

Fig. 4 (a) Variation of the molar magnetic susceptibility *vs.* temperature for $x = 0.05$, 0.10, and 0.15 phases. (b) Variation of magnetization with the magnetic field at 2 K for the $x = 0.05$ and $x = 0.10$ compounds.

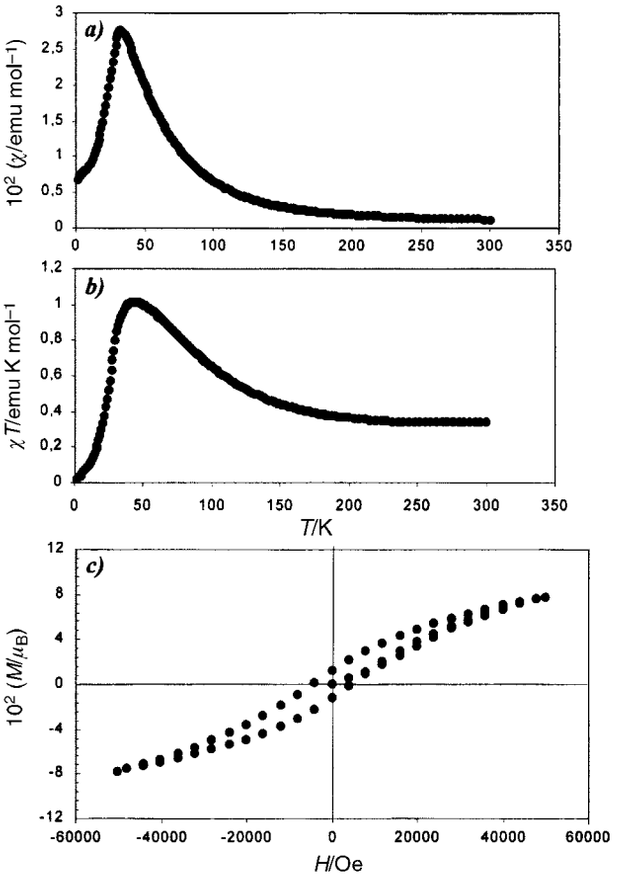

Fig. 5 Magnetic behaviour of $LaNi_{0.80}Mo_{0.20}O_3$: (a) variation of the magnetic susceptibility with the temperature; (b) variation of χT *vs.* T at 1000 Oe; (c) variation of magnetization with the magnetic field at 2 K.

~150 K. This fact suggests that electronic localization now occurs in these systems, becoming greater as the x value increases (*i.e.* as the amount of Ni^{2+} is increased). This fact agrees well with the electrical resistivity measurements previously discussed, since the conductivity values progressively decrease as x increases. On the other hand, one observes a maximum above 40 K which is clearer for $x = 0.15$, indicative of antiferromagnetic interactions.

In order to confirm the above assumptions about the magnetic behaviour of these materials, the variation of magnetization against the magnetic field has been measured. No hysteresis loops are detected at temperatures above 2 K but, at this temperature, in the sample $x = 0.05$ a weak loop is suggested (Fig. 4(b)), but it is not observable for $x = 0.10$ and $x = 0.15$.

Some noticeable features arise in the magnetic behaviour of the most substituted phase, $x = 0.20$, for which the susceptibility results are displayed in Fig. 5(a) in the temperature range 2–300 K. This quantity increases when the temperature decreases, showing a transition at 100 K, and reaching a sharp maximum at 34 K, for which the susceptibility reaches a value of 0.027 emu mol^{-1}. In the same sense, the plot of χT *vs.* T, Fig. 5(b), shows a significant increase up to about 30 K and then falls sharply as the temperature decreases. This fact indicates that the dominant magnetic exchange interactions are antiferromagnetic in nature.[21] However, the increase of the magnetization below 100 K can be attributed to short-range magnetic ordering on a weakly ferromagnetic component. This quite interesting magnetic behaviour of the sample with $x = 0.20$ led us to undertake a more detailed study on the field-dependent magnetization at 2 K (Fig. 5(c)). A ferromagnetically ordered component is clearly revealed by the observation of the hysteresis loops (note the difference of one order of magnitude in the ordinate scale with respect to

Table 3 Magnetic parameters for $LaNi_{0.80}Mo_{0.20}O_3$: saturation magnetization (M_s), remanent magnetization (M_R) and coercive field (H_c)

T/K	M_s/μ_B Ni^{-1}	M_R/μ_B Ni^{-1}	H_c/Oe
2	3.5×10^{-2}	1.161×10^{-2}	4000

Fig. 4(b)). Table 3 gathers the most representative magnetic parameters obtained for this phase.

An important feature is that the induced moments seen in these isothermal magnetization curves are very low, suggesting a weak correlated ferromagnetic moment. This fact indicates that the antiferromagnetic and ferromagnetic ordering take place simultaneously. The observed behaviour could therefore be explained assuming an antiferromagnetic spin arrangement with a small ferromagnetic canting of the order of 0.03 μ_B. Similar results have previously been interpreted in relation to the existence of non-collinear spin structures.[12]

In conclusion, we have synthesized the series $LaNi_{1-x}Mo_xO_3$ ($0.05 \leqslant x \leqslant 0.20$) that adopts two different symmetries depending on the degree of substitution, x. The actual composition of the samples also drives their electrical and magnetic behaviour, that varies from metal-like ($x = 0.05$–0.15) to semiconductor ($x = 0.20$) and from weakly ferromagnetic ($x = 0.05$) to antiferromagnetic with very weak ferromagnetic canting ($x = 0.20$), respectively.

Acknowledgements

Financial support from CICYT, Spain (Grant No. MAT97-0326-C04-03) is gratefully acknowledged. We thank ILL (Grenoble, France) for the availability of their installations.

References

1 J. A. Alonso, M. J. Martínez-Lope, M. T. Casais, J. L. García-Muñoz and M. T. Fernández-Díaz, *Phys. Rev. B*, 2000, **61**(3), 1756.
2 J. A. Alonso, J. L. García-Muñoz, M. T. Fernández-Díaz, M. A. G. Aranda, M. J. Martínez-Lope and M. T. Casais, *Phys. Rev. Lett.*, 1999, **82**(19), 3871.
3 M. Medarde, *J. Phys. Condens. Matter*, 1997, **9**, 1679.
4 M. Medarde, P. Lacorre, K. Conder, F. Fauth and A. Furrer, *Phys. Rev. Lett.*, 1998, **80**, 2397.
5 J. B. Torrance, P. Lacorre, A. I. Nazzal, E. J. Ansaldo and Ch. Niedermayer, *Phys. Rev. B*, 1992, **45**, 8209.
6 J. L. García Muñoz, J. Rodríguez Carvajal, P. Lacorre and J. B. Torrance, *Phys. Rev. B*, 1992, **46**, 4414.
7 Z. Zhang and M. Greenblatt, *J. Solid State Chem.*, 1994, **111**, 145.
8 I. Álvarez, M. L. Veiga and C. Pico, *J. Solid State Chem.*, 1998, **136**, 313.
9 P. D. Battle and J. F. Vente, *J. Solid State Chem.*, 1999, **146**, 163.
10 K. Sreedhar and J. M. Honig, *J. Solid State Chem.*, 1994, **111**, 147.
11 I. Álvarez, J. L. Martínez, M. L. Veiga and C. Pico, *J. Solid State Chem.*, 1996, **125**, 47.
12 I. Álvarez, M. T. Fernández-Díaz, J. L. Martínez, M. L. Veiga and C. Pico, *J. Solid State Chem.*, 1997, **134**, 274.
13 I. Álvarez, M. L. Veiga and C. Pico, *J. Mater. Chem.*, 1995, **5**(7), 1049.
14 E. Rodríguez, I. Álvarez, M. L. López, M. L. Veiga and C. Pico, *J. Solid State Chem.*, 1999, **148**, 479.
15 M. Pechini, *U.S. Pat.* 3, 231, 1966.
16 J. Rodríguez-Carvajal, *Physica B (Amsterdam)*, 1993, **192**, 55.
17 L. J. Van der Pauw, *Philips Res. Rep.*, 1958, **1**, 13.
18 K. P. Rajeev, G. V. Shivashankar and A. K. Raychaudhuri, *Solid State Commun.*, 1991, **79**(7), 591.
19 J. B. Torrance, P. Lacorre, C. Asavaroenghai and R. M. Metzger, *J. Solid State Chem.*, 1991, **90**, 168.
20 K. Sreedhar, J. M. Honig, M. Darwin, M. McElfresh, P. M. Shand, J. Xu, B. C. Crooker and J. Spalek, *Phys. Rev. B*, 1992, **46**(10), 6382.
21 *Magnetism and Chemical Bond*, ed. J. B. Goodenough, R. E. Krieger, New York, 1976.